GLUCOSAMINE INOSITOLPHOSPHORYLCERAMIDE TRANSFERASE1 (GINT1) Is a GlcNAc-Containing Glycosylinositol Phosphorylceramide Glycosyltransferase[1][OPEN]

Toshiki Ishikawa,[a,2] Lin Fang,[b,c,2,3] Emilie A. Rennie,[c,d,e,4] Julien Sechet,[b,c] Jingwei Yan,[b,c,5] Beibei Jing,[b,c] William Moore,[b,c,d] Edgar B. Cahoon,[e] Henrik V. Scheller,[b,c,d] Maki Kawai-Yamada,[a] and Jenny C. Mortimer[b,c,6]

[a]Graduate School of Science and Engineering, Saitama University, Saitama 338-8570, Japan
[b]Joint BioEnergy Institute, Emeryville, California 94608
[c]Biosciences Area, Lawrence Berkeley National Laboratory, Berkeley, California 94720
[d]Department of Plant and Molecular Biology, University of California, Berkeley, California 94720
[e]Center for Plant Science Innovation and Department of Biochemistry, University of Nebraska-Lincoln, Lincoln, Nebraska 68588

ORCID IDs: 0000-0001-8083-6542 (T.I.); 0000-0002-9971-4569 (L.F.); 0000-0002-4115-356X (E.A.R.) (E.A.R.); 0000-0001-8398-4743 (J.S.); 0000-0003-4930-0875 (J.Y.); 0000-0002-9421-5701 (B.J.); 0000-0002-1140-7661 (W.M.); 0000-0002-7277-1176 (E.B.C.); 0000-0002-6702-3560 (H.V.S.); 0000-0002-8732-052X (M.K.) (M.K.); 0000-0001-6624-636X (J.C.M.) (J.C.M.)

Glycosylinositol phosphorylceramides (GIPCs), which have a ceramide core linked to a glycan headgroup of varying structures, are the major sphingolipids in the plant plasma membrane. Recently, we identified the major biosynthetic genes for GIPC glycosylation in Arabidopsis (*Arabidopsis thaliana*) and demonstrated that the glycan headgroup is essential for plant viability. However, the function of GIPCs and the significance of their structural variation are poorly understood. Here, we characterized the Arabidopsis glycosyltransferase GLUCOSAMINE INOSITOLPHOSPHORYLCERAMIDE TRANSFERASE1 (GINT1) and showed that it is responsible for the glycosylation of a subgroup of GIPCs found in seeds and pollen that contain GlcNAc and GlcN [collectively GlcN(Ac)]. In Arabidopsis *gint1* plants, loss of the GlcN(Ac) GIPCs did not affect vegetative growth, although seed germination was less sensitive to abiotic stress than in wild-type plants. However, in rice, where GlcN(Ac) containing GIPCs are the major GIPC subgroup in vegetative tissue, loss of GINT1 was seedling lethal. Furthermore, we could produce, de novo, "rice-like" GlcN(Ac) GIPCs in Arabidopsis leaves, which allowed us to test the function of different sugars in the GIPC headgroup. This study describes a monocot GIPC biosynthetic enzyme and shows that its Arabidopsis homolog has the same biochemical function. We also identify a possible role for GIPCs in maintaining cell-cell adhesion.

Plant sphingolipids are highly complex, diverse structural lipids. Glycosylinositol phosphorylceramides (GIPCs) represent the major sphingolipids in the plant plasma membrane. Approximately 64% of sphingolipids and ~25% of total plasma membrane lipids are GIPCs, which interact with sterols to form membrane microdomains (Markham and Jaworski, 2007; Cacas et al., 2016). Besides serving as a membrane structural component, GIPCs are bioactive molecules involved in cell signaling and regulation (Dunn et al., 2004).

The core structure of plant GIPCs consists of inositol phosphorylceramide (IPC) linked to GlcA. Additional sugar units can be added, such as glucosamine (GlcN), *N*-acetyl-glucosamine (GlcNAc), Man, Gal, and arabinose (Markham et al., 2006, 2013; Buré et al., 2011). The glycan patterns vary among plant species and tissues, indicating that different GIPC glycosylation pathways and enzymes are involved. Generally, there are two types of glycan structure: hexose(s) linked to GlcA-IPC in Arabidopsis (*Arabidopsis thaliana*) vegetative tissue and GlcN(Ac) linked to GlcA-IPC in rice (*Oryza sativa*), tobacco (*Nicotiana tabacum*), and reproductive tissues (seeds and pollen) of Arabidopsis, as shown in Figure 1.

The headgroup structure and biosynthesis of plant GIPCs has not been fully elucidated. However, recently, characterization of GIPC biosynthetic enzymes was reported (Fig. 1). GIPCs are initially formed by the addition of an inositol phosphate to the ceramide through the action of IPC synthase (Wang et al., 2008). IPCs then go through several glycosylation steps in the Golgi. INOSITOL PHOSPHORYLCERAMIDE GLUCURONOSYLTRANSFERASE1 (IPUT1), the first glycosyltransferase (GT) identified, transfers GlcA from UDP-GlcA to IPC (Rennie et al., 2014), forming GlcA-IPC. GOLGI-LOCALIZED NUCLEOTIDE SUGAR TRANSPORTER1 (GONST1) is responsible for importing GDP-Man into the Golgi specifically for GIPC biosynthesis, and GIPC MANNOSYL-TRANSFERASE1 (GMT1) uses this substrate to transfer Man onto GlcA-IPC (Mortimer et al., 2013; Fang et al., 2016). *gmt1*, *gonst1*, and pollen-rescued *iput1* show severe dwarfism and constitutive accumulation of salicylic acid, suggesting that the headgroup plays an important role in plant growth and development, as well as in

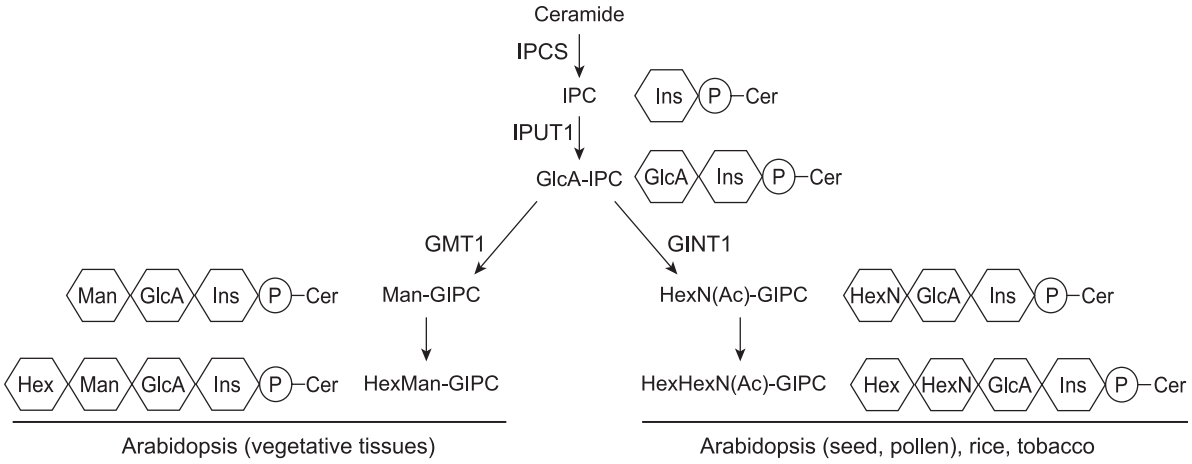

Figure 1. Representative structures and synthetic pathways of GIPC sugar headgroups in plants. The first (Ins) and second (GlcA) carbohydrate residues are conserved in plants, but the third residue (Hex, HexN, or HexNAc) is variable in plant tissues/species. This study identifies the (*N*-acetyl)hexosamine-specific transferase GINT1. IPCS, inositolphosphorylceramide synthase (ceramide phosphoinosityl transferase); IPUT1, inositolphosphorylceramide glucuronosyl transferase; GMT1, GIPC mannosyl transferase; P, phosphate group; Ins, inositol; Cer, ceramide.

defense responses (Mortimer et al., 2013; Fang et al., 2016; Tartaglio et al., 2017). More recently, we showed that the headgroup of GIPCs can serve as the binding site for pathogenic toxins and as a result determine the host selectivity of some classes of plant pathogens (Lenarčič et al., 2017).

In this work, we characterized the GT64 protein GLUCOSAMINE INOSITOLPHOSPHORYLCERAMIDE TRANSFERASE1 (GINT1) and showed that it is responsible for the addition of GlcNAc to GIPCs. In Arabidopsis, in which GlcN(Ac)-containing GIPCs are dominant in seeds and pollen (Luttgeharm et al., 2015), *gint1* plants grow normally under standard conditions. However, GlcN(Ac)-containing GIPCs are the dominant form in almost all tissue types in rice, and loss of OsGINT1 results in seedling lethality.

RESULTS

Identification of a Putative GIPC GT in GT64

We recently characterized AtGMT1 (At3g55830), a member of the Arabidopsis CAZy GT64 family, as a GIPC mannosyltransferase (Fang et al., 2016). Here, we chose to investigate At5g04500, the homolog of AtGMT1, which we now propose to rename *GLUCOSAMINE INOSITOLPHOSPHORYLCERAMIDE TRANSFERASE1* (*AtGINT1*). The GT64 family has three members in Arabidopsis, which show low percentage sequence similarity to each other (29% shared sequence identity between AtGMT1 and AtGINT1; Fang et al., 2016). AtGINT1 is 767 amino acids long (compared to AtGMT1, which is 334 amino acids) and has orthologs across the plant kingdom, from charophyte to angiosperms (Supplemental Fig. S1). AtGINT1 also contains a predicted exostosin (EXT) domain (Inter-Pro; Finn et al., 2017). In humans, EXTs have both a GT64 and a GT47 domain and are required for the biosynthesis of heparan-sulfate, a glycosaminoglycan, in which the major repeating disaccharide unit consists of GlcA linked to GlcNAc (Busse-Wicher et al., 2014). The GT64 domain in EXT is responsible for the transfer of GlcNAc from UDP-GlcNAc to GlcA. Recently, it was shown that some Arabidopsis tissues contain

[1]This work was part of the Department of Energy Joint BioEnergy Institute supported by the U.S. Department of Energy, Office of Science, Office of Biological and Environmental Research, through contract DE-AC02-05CH11231 between Lawrence Berkeley National Laboratory and the U.S. Department of Energy. E.A.R. was supported by a Life Sciences Research Foundation fellowship from the Gordon and Betty Moore Foundation. This work was also supported by the Japan Society for the Promotion of Science (KAKENHI grants 17K15411 and 26292190 to T.I. and M.K.-Y.) and by the National Science Foundation (MCB-1158500 to E.B.C.).

[2]These authors contributed equally to the article.

[3]Current address: South China Botanical Garden, Chinese Academy of Sciences, Guangzhou 510650, China.

[4]Current address: Callisto Media, Emeryville, California 94608.

[5]Current address: College of Life Sciences, Nanjing Agricultural University, Nanjing, Jiangsu 210095, China.

[6]Address correspondence to jcmortimer@lbl.gov.

The author responsible for distribution of materials integral to the findings presented in this article in accordance with the policy described in the Instructions for Authors (www.plantphysiol.org) is: Jenny C. Mortimer (jcmortimer@lbl.gov).

T.I., L.F., E.A.R., and J.C.M. designed the research; T.L., L.F., E.A.R., J.S., J.Y., B.J., and W.M. performed research; T.I., L.F., E.A.R., M.K.-Y., H.V.S., E.B.C., and J.C.M. analyzed the data; J.C.M., L.F., and T.I. wrote the article.

[OPEN]Articles can be viewed without a subscription.

www.plantphysiol.org/cgi/doi/10.1104/pp.18.00396

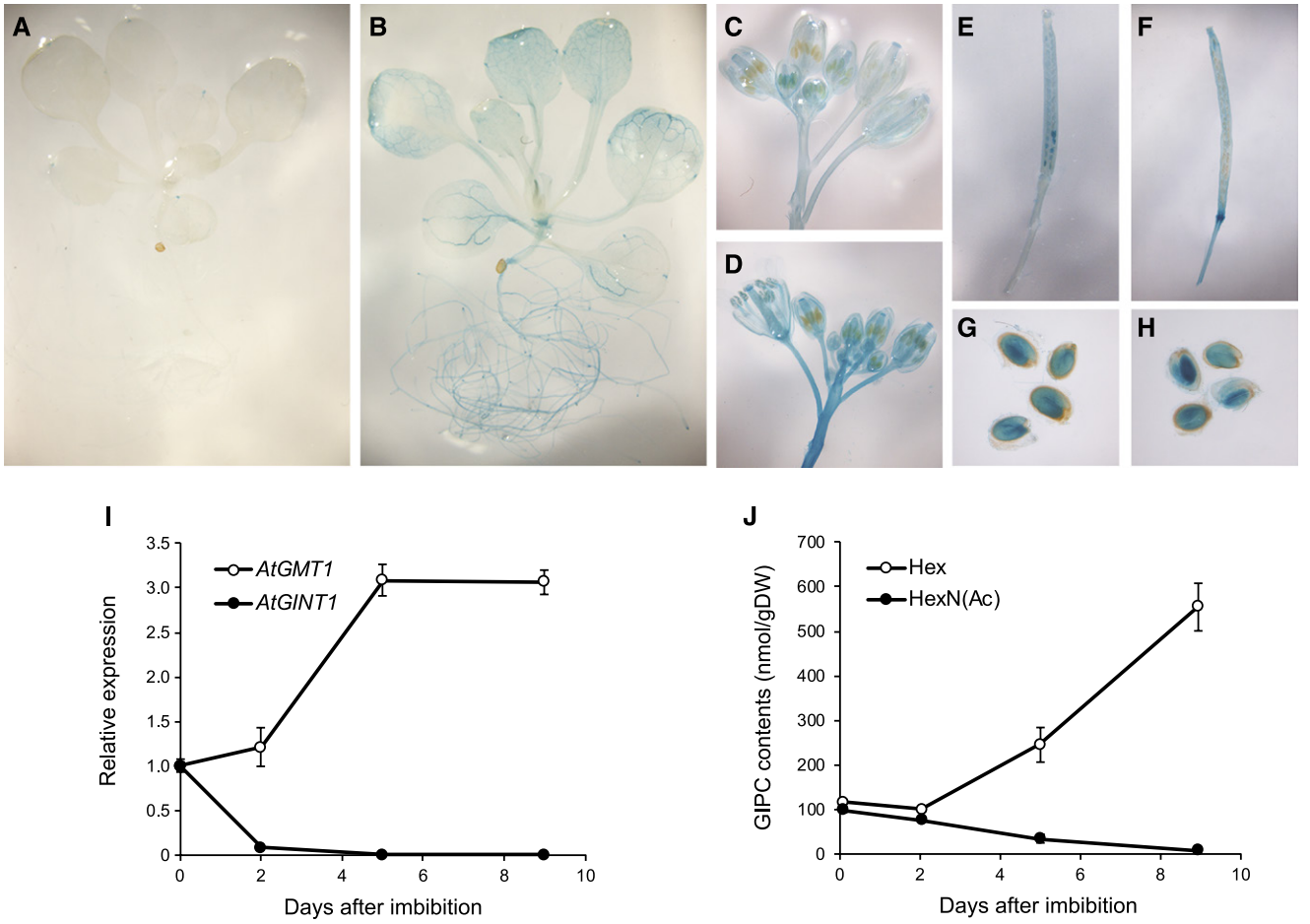

Figure 2. Tissue-specific expression of *AtGINT1* and *AtGMT1* and comparison of GIPC subclasses. A to H, Promoter-GUS staining indicating expression patterns of *AtGINT1* (A, C, E, and G) and *AtGMT1* (B, D, F, and H) in young seedlings (A and B), flowers (C and D), developing siliques (E and F), and mature seeds (G and H). I and J, GT expression analysis (I) and quantification of GIPC contents (J) during seed germination. Data are means of three or four biological replicates ± SD.

GIPCs that have an IPC core linked to a GlcA (GlcA-IPC) linked to a GlcN(Ac) [GlcN(Ac)-GlcA-IPC; Fig. 1; Tellier et al., 2014; Luttgeharm et al., 2015]. Therefore, we considered AtGINT1 a good candidate for the GT responsible for the addition of GlcNAc to GlcA-IPC in these tissues.

Tissue-Specific Expression in Arabidopsis

GlcN(Ac)-containing GIPCs are most abundant in Arabidopsis seeds and undetectable in vegetative tissue (Tellier et al., 2014), and therefore we predicted that *AtGINT1* gene expression should reflect this. Both publicly available microarray data (Supplemental Fig. S2, B and C; Winter et al., 2007) and expression of a reporter construct containing *Escherichia coli β-GLUCURONIDASE* driven by the *AtGINT1* promoter ($GINT1_{pro}$:*GUS*; Fig. 2; Supplemental Fig. S2, D and E) showed that *AtGINT1* is specifically and highly expressed in the developing embryo and mature seed. Almost no signal was observed in vegetative tissues, but weak GUS staining was detected in stigma and pollen (Fig. 2), consistent with the presence of GlcN(Ac)-containing GIPCs in flowers (Fig. 3) and pollen (Luttgeharm et al., 2015). In contrast, *AtGMT1*, the predominant GIPC mannosyl transferase (Fang et al., 2016), was expressed in all tissues, in accordance with the ubiquitous distribution of Hex-GlcA-IPCs in Arabidopsis. Reverse transcription quantitative PCR (RT-qPCR) and sphingolipidomic analysis also demonstrated the correlation of transcriptional levels of the two putative sugar transferases and the composition of the GIPC sugar headgroup in seed and germinating seedlings. *AtGINT1* was highly expressed in dry seed but drastically downregulated after seed imbibition in parallel with a rapid decline of HexN(Ac)-containing GIPC content, whereas the levels of *AtGMT1* transcript and Hex-GIPCs were synchronously elevated during seed germination (Fig. 2).

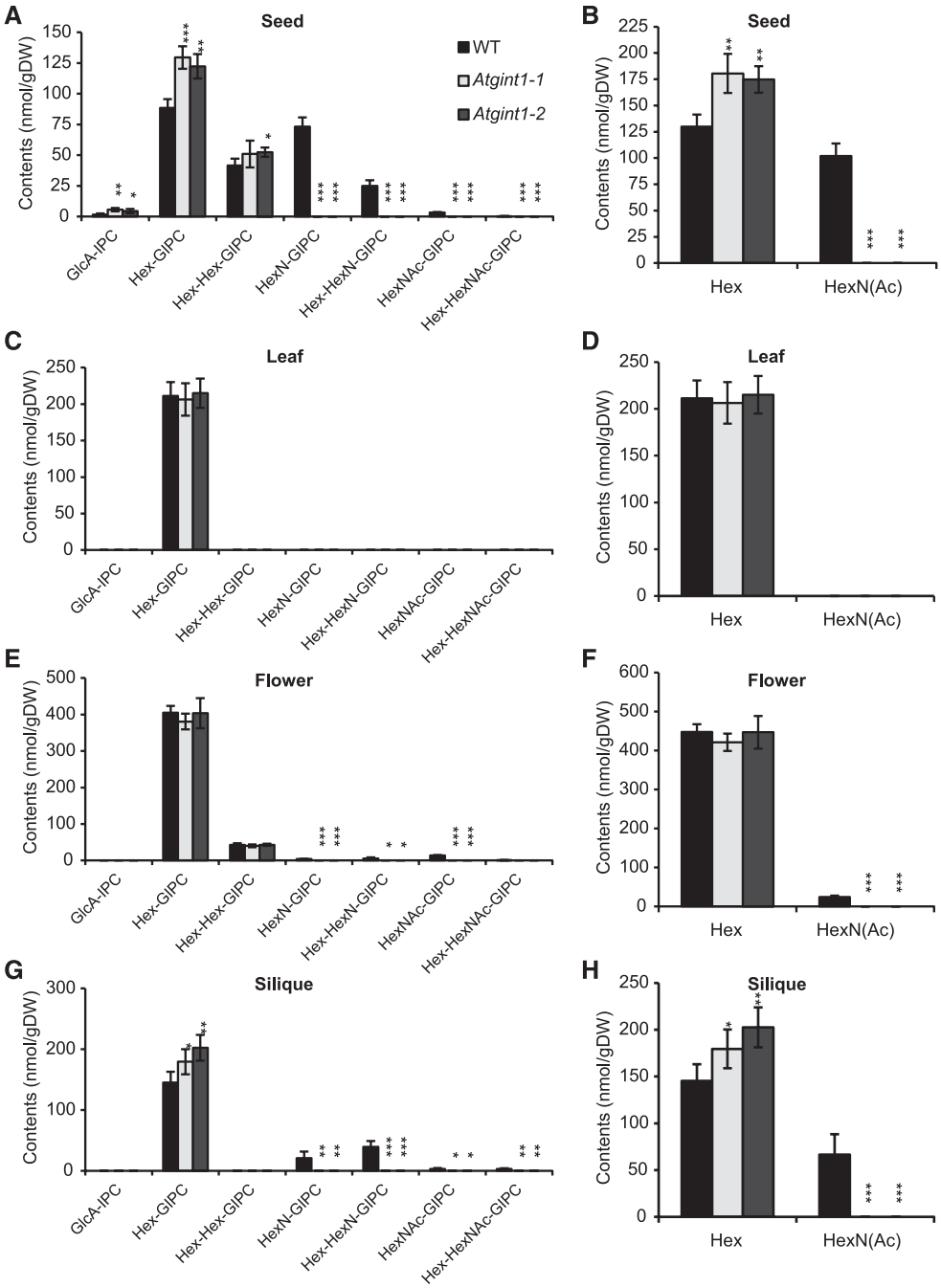

Figure 3. GIPC composition of *Atgint1* plants. A to H, LC-MS/MS was used to determine the GIPC composition of dry seeds (A and B), leaves of 3-week-old plants (C and D), flowers (E and F), and developing green siliques (G and H). A, C, E, and G, Accumulation profiles of all the major GIPC classes. B, D, F, and H, Overall amounts of either Hex_n-only GIPCs (Hex) or HexN(Ac)-containing GIPCs [HexN(Ac)]. Data are means of three biological replicates ± SD. Asterisks indicate significant difference compared to that in the wild type (Student's *t* test, $*P < 0.05$, $**P < 0.01$, $***P < 0.001$).

Isolation of Arabidopsis T-DNA Lines

We next obtained two allelic T-DNA insertion mutants, *Atgint1-1* (SALK_002825) and *Atgint1-2* (GK_834G06), both in the Columbia-0 (Col-0) ecotype background (Supplemental Fig. S3A). We isolated plants homozygous for the T-DNA insertion, confirmed the location of the insertions by sequencing, and showed that both alleles lacked detectable *AtGINT1* transcript by RT-PCR (Supplemental Fig. S3B). Both mutants grew normally on agar and soil under standard conditions and showed no gross morphological phenotype compared to that of wild type.

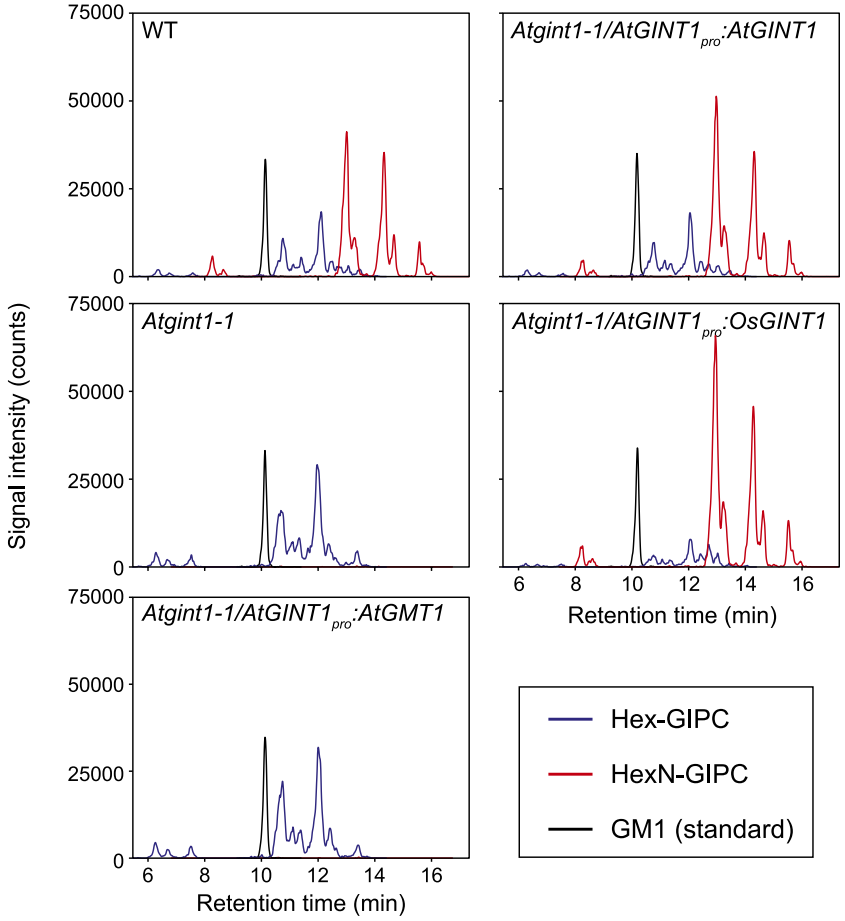

Figure 4. Complementation of the HexN-GIPC deficiency in *Atgint1*. LC-MS/MS chromatograms of the dry seed sphingolipidome in *Atgint1-1*, *Atgint1-1* expressing $AtGINT1_{pro}$:*AtGINT1*, $AtGINT1_{pro}$:*OsGINT1*, and $AtGINT1_{pro}$:*AtGMT1*. Total ion counts corresponding to Hex-GIPCs (blue line), HexN-GIPCs (red line), and Ganglioside GM1 (internal standard, black line) are shown.

Analysis of GIPCs in *Atgint1* Plants

Next, we analyzed GIPC composition by sphingolipidomics using multiple reaction monitoring liquid chromatography-tandem mass spectrometry (LC-MS/MS; Fang et al., 2016; Ishikawa et al., 2016), which is necessary to survey the extensive variation in both the ceramide moiety and the type and degree of glycosylation attached to the GlcA-IPC core. GIPCs from Arabidopsis leaves are almost exclusively composed of Hex-GlcA-IPCs, but those from flowers, siliques, and seeds also contain HexN(Ac)-GlcA-IPCs in wild-type plants (Fig. 3; Supplemental Data Set 1). In *Atgint1* plants, HexN(Ac)-GlcA-IPCs were undetectable in these tissues, whereas Hex-GlcA-IPCs accumulated in siliques and seeds at significantly higher levels than in wild-type plants. No significant differences in the ceramide and glucosylceramide fractions were observed between *Atgint1* and wild type (Supplemental Fig. S4). It should be noted that *AtGMT1* expression levels did not change in *Atgint1* (Supplemental Fig. S5) and that GlcA-IPC did not accumulate. These data suggest that AtGINT1 is a HexNAc-specific GIPC sugar transferase.

Complementation of *Atgint1* by *GINT1* Expression

To evaluate the hypothesized difference in substrate specificity between AtGINT1 and AtGMT1, we prepared heterologous complementation lines by expressing $AtGINT1_{pro}$:*AtGINT1* and $AtGINT1_{pro}$:*GMT1* in *Atgint1-1*. The loss of HexN(Ac)-GIPCs in dry seeds was completely recovered in genomic *AtGINT1*-complemented lines. The rice *AtGINT1* homolog, *OsGINT1*, also rescued the deficiency, whereas expression of *AtGMT1* did not rescue the phenotype in any of the independent transgenic lines tested (Fig. 4).

Since HexN(Ac)-containing GIPCs are undetectable in Arabidopsis vegetative tissue, we expressed *AtGINT1* and *OsGINT1* in wild-type Arabidopsis plants, driven by the cauliflower mosaic virus (CaMV) 35S constitutive promoter ($35S_{pro}$) (Fig. 5). In both cases, we could now successfully detect HexN(Ac)-GIPCs in leaf tissue by LC-MS/MS (Fig. 5A). These transgenic plants did not show any visible phenotypes, probably because the comparatively low levels of HexN(Ac)-GIPC (~4 mol% for *35Spro:AtGINT1* and ~20 mol% for *35Spro:OsGINT1*), and the unchanged Hex-GIPC levels (Fig. 5B).

Phenotype of *Atgint1* Seeds

Since GlcN(Ac)-GlcA-IPCs are highly enriched in Arabidopsis seeds and *AtGINT1* is specifically expressed in developing embryos and seeds, we investigated how the loss of *AtGINT1* might affect seed morphology and germination.

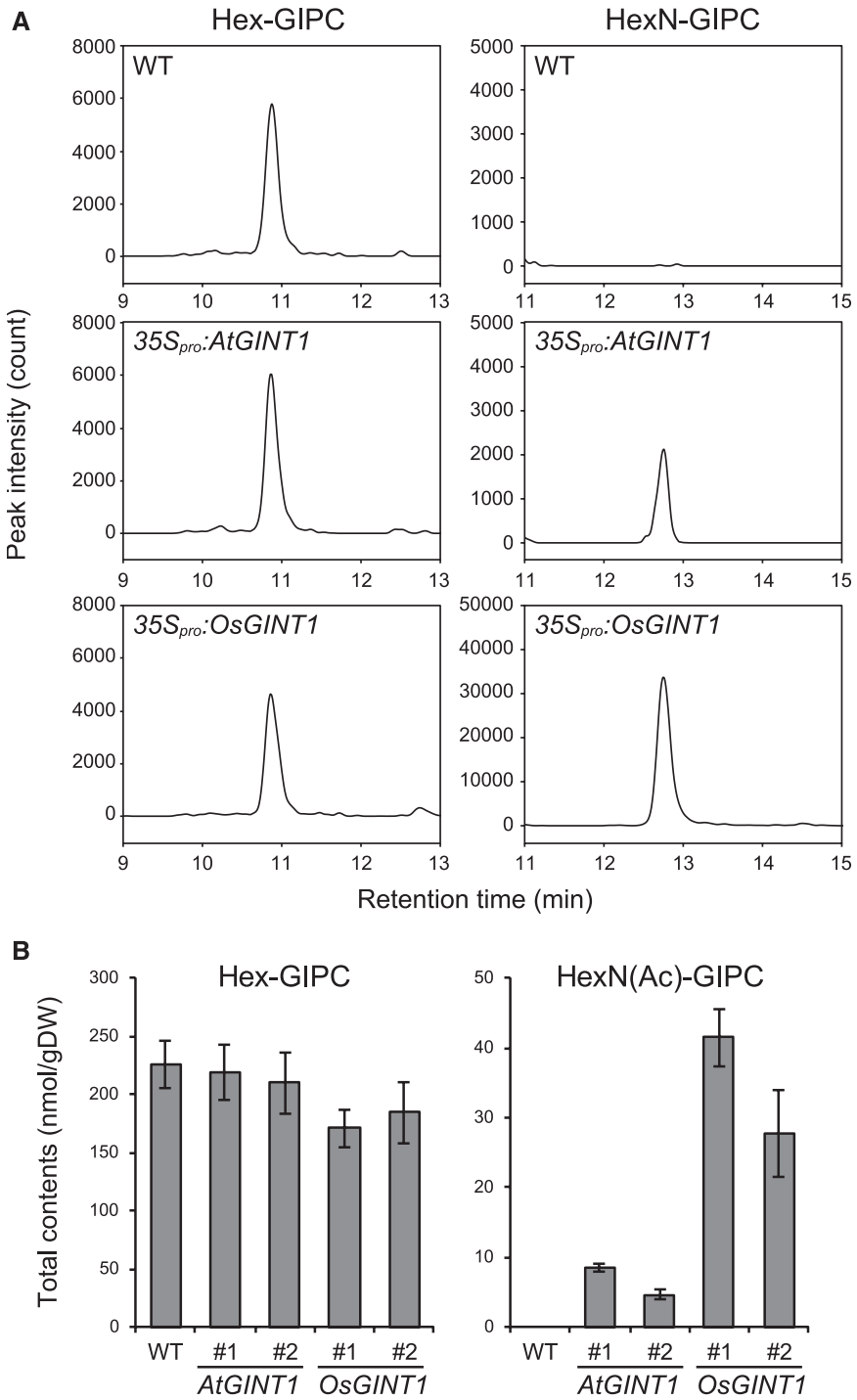

Figure 5. De novo synthesis of HexN-GlcA-IPCs in Arabidopsis leaves following constitutive expression of *AtGINT1* or *OsGINT1*. A, LC-MS/MS chromatograms of Hex-GIPC (t18:1-h24:1, left) and HexN-GIPC (t18:1-h24:1, right) are shown. B, Total quantity of HexN- and HexN(Ac)-GIPC in leaves of Arabidopsis expressing *35Spro:AtGINT1* or *35Spro:OsGINT1*.

First, we investigated mucilage production. During imbibition, Arabidopsis seed coat cells produce a large quantity of mucilage, which can be visualized using ruthenium red staining (Fig. 6A). This was unaffected in the *Atgint1* seeds. We then used scanning electron microscopy to investigate the seed coat in more detail. The seed coat of *Atgint1* seeds appeared normal (Fig. 6C), although the seeds were slightly larger. Indeed, the *Atgint1* seeds are significantly heavier (Fig. 6E) and have a significant increase in seed storage lipid (Fig. 6F) and protein content (Fig. 6G). Transmission electron microscopy (TEM) revealed that *Atgint1* seed coat cells are slightly larger than those of the wild type (Fig. 6D) but had a normal distribution of oil and starch bodies. Examination of developing siliques did not reveal abnormal embryo development (Supplemental Table S1).

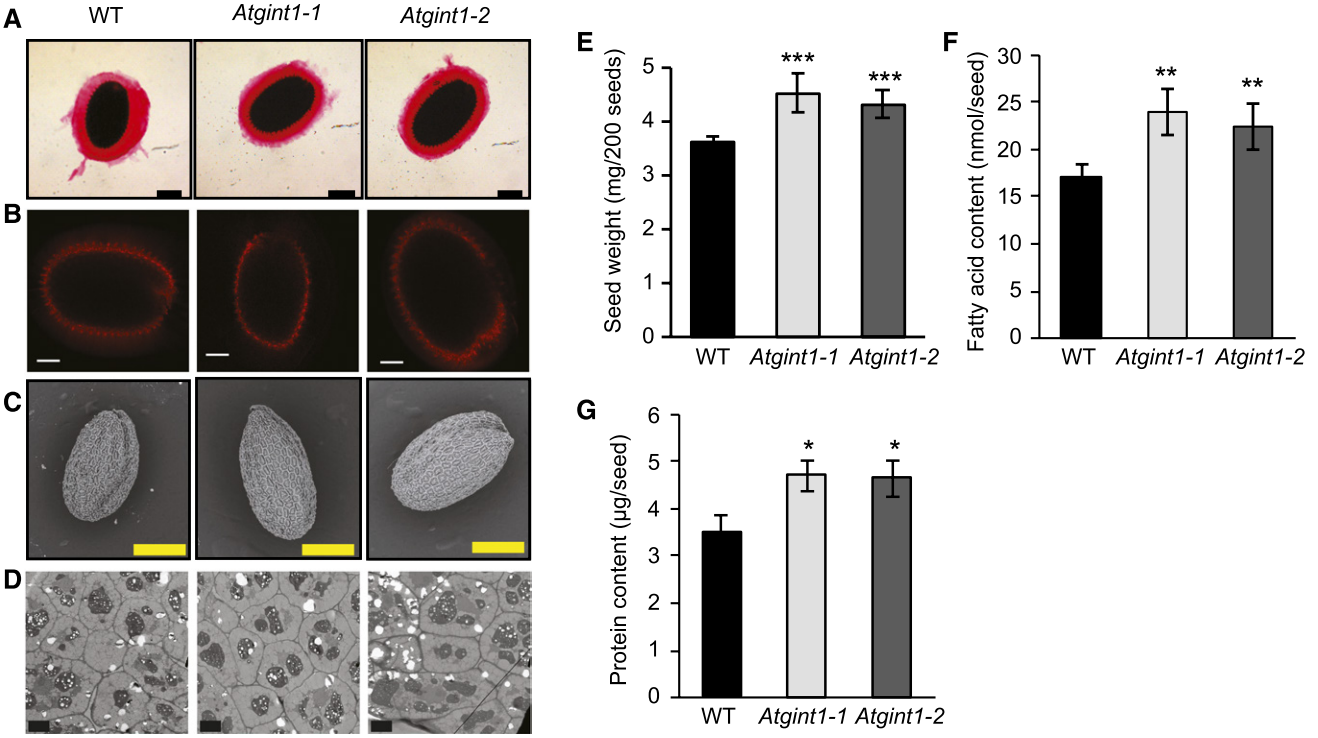

Figure 6. Microscopy analysis and cell wall composition of wild-type and *Atgint1* seeds. A, Ruthenium red staining of imbibed seeds indicating mucilage layer. Bar = 200 µm. B, Scarlet4B staining of imbibed seeds indicating cellulose rays in mucilage. Bar = 100 µm. C, Scanning electron microscopy. Bar = 200 µm. D, TEM. Bar = 4 µm. E, Seed weight. F, Seed fatty acid content. G, Seed protein content. A to D, representative images are shown. E to G, Data are means of 3 or 4 biological replicates ± SD. Asterisks indicate significant difference compared to the wild type (Student's *t* test, $*P < 0.05$, $**P < 0.01$, $***P < 0.001$).

Both Cellulosic and Noncellulosic Cell Wall Polysaccharides Are Unaffected in *Atgint1*

Previously, we showed that *Atgmt1* had reduced crystalline cellulose, but an otherwise unchanged cell wall composition (Fang et al., 2016). To see if the loss of AtGINT1 impacted the seed cell wall, we prepared destarched alcohol insoluble residue (AIR) from dry seeds. We then performed trifluoroacetic acid (TFA) hydrolysis to release the noncellulosic monosaccharides, which were quantified by high performance anion-exchange chromatography-pulsed amperometric detection (Fig. 7; Supplemental Data Set 2). No significant difference was detected between *Atgint1* and the wild type (Fig. 7A). The TFA-insoluble residue was then further hydrolyzed using sulfuric acid to release the Glc from cellulose. No significant difference from the wild type was detected for mutant lines carrying either *Atgint1* allele (Fig. 7B). Since cell-specific variation in polysaccharide composition may be masked when using these bulk analysis techniques, we also used Scarlet4B staining to investigate the production of cellulose rays in the mucilage of the germinating seeds (Fig. 6B). Again, these were normal in the *Atgint1* seeds.

Although *AtGINT1* is expressed mainly in the developing seed (Supplemental Fig. S2), we also tested the cell wall composition of vegetative tissues. However, there were no significant changes in the cell wall composition of *Atgint1* mature stems and young leaves compared to that of the wild type (Supplemental Fig. S6; Fig. 7B).

Germination of *Atgint1* Seeds Is Resistant to Abscisic Acid and Salt

To further explore the possible functional role for GlcN(Ac)-GIPCs in Arabidopsis seeds, we explored *Atgint1* germination rates under various growth conditions. Under standard conditions, there was no significant difference between wild-type and *Atgint1* germination (Supplemental Fig. S7; Fig. 8). Next, we tested whether mimicking ageing, via storage of seeds in high humidity and temperature, differentially affected germination (Supplemental Fig. S7). Again, no significant difference was seen.

The plant hormone abscisic acid (ABA) inhibits radicle growth emergence in imbibed seeds. Previous work has shown that Arabidopsis plants with a partial loss of SPHINGOSINE KINASE1 were less sensitive to application of exogenous ABA (Worrall et al., 2008). The *Atgint1* seeds showed a similar phenotype with significantly higher germination than wild-type seeds when germinated on 0.5× Murashige and Skoog media

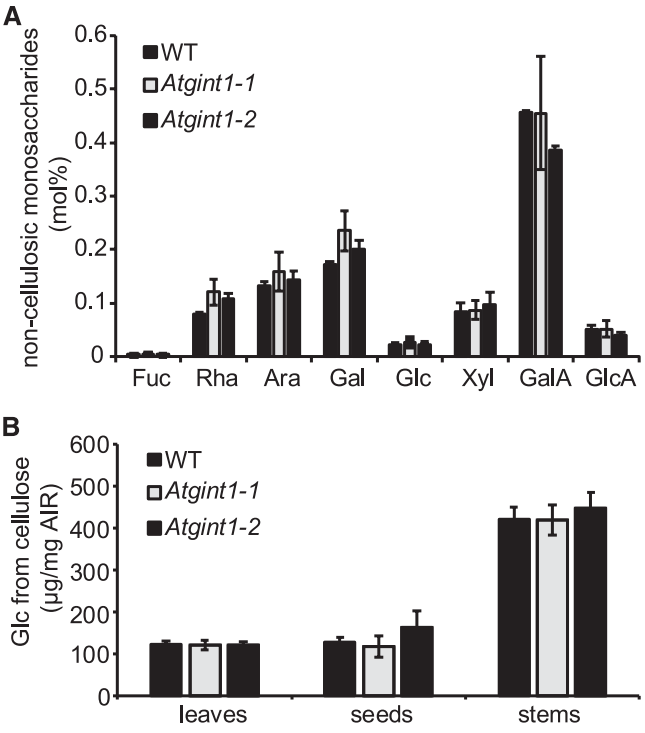

Figure 7. Cell wall composition of *Atgint1*. A, Monosaccharide composition of seed AIR following TFA hydrolysis. B, Glc released from TFA-insoluble AIR from leaves, stems, and seeds following Saeman hydrolysis. Data are means of three biological replicates ± SD. No statistically significant difference (Student's *t* test, $P < 0.05$) was observed between wild-type and *Atgint1* plants.

containing either 0.5, 1, or 2.5 µM ABA (Fig. 8A). Since ABA-insensitive mutants can have reduced sensitivity to salinity during germination, we also tested whether this was the case with *Atgint1-1* and *Atgint1-2*. Indeed, both mutant lines had significantly higher germination rates than the wild type in the presence of 100 and 125 mM NaCl, although this difference was lost at the highest NaCl concentration tested (Fig. 8B).

OsGINT1 Is Responsible for HexN(Ac)-GIPC Synthesis and Normal Growth in Rice

GINT1 expression and HexN(Ac)-GIPC production are tissue-specific in Arabidopsis, in contrast to the ubiquitous presence of Hex-GIPCs produced by AtGMT1. In rice, on the other hand, *OsGINT1* is highly expressed in almost all tissues, whereas *OsGMT1* expression is barely detectable (Supplemental Fig. S8), which corresponds with the distribution of the respective GIPC head group in rice, i.e. HexN(Ac)-GIPCs are ubiquitous but Hex-GIPCs are undetectable in most tissues (Ishikawa et al., 2016).

To test the function of HexN(Ac)-GIPCs in rice, we used the CRISPR/Cas9 gene-editing tool to disrupt *OsGINT1* using two different target sequences (Supplemental Fig. S9). Most transgenic calli grew as well as the wild type, but upon transfer of calli to regeneration medium followed by transfer to rooting medium, some shoots became stunted and eventually died (Fig. 9A). Sphingolipidomic analysis of the regenerated shoots revealed that wild-type shoots and transgenic shoots with a normal growth phenotype had wild-type levels of HexN(Ac)-GIPCs present (Fig. 9B). However, regenerated shoots with abnormal growth displayed a drastic reduction in HexN(Ac)-GIPCs, as well as an accumulation of GlcA-IPCs, the proposed substrate of GINT1/GMT1 (Fig. 9B).

This corresponds to the observations from *Atgmt1*, which also accumulates GlcA-IPCs (Fang et al., 2016). It should be noted that *Atgmt1* also grows well on callus-inducing medium (Fang et al., 2016) but fails to regenerate on shoot-inducing medium (Supplemental Fig. S10). These results indicate indispensable roles for the predominant GIPC head groups, specifically Hex in Arabidopsis and HexN(Ac) in rice.

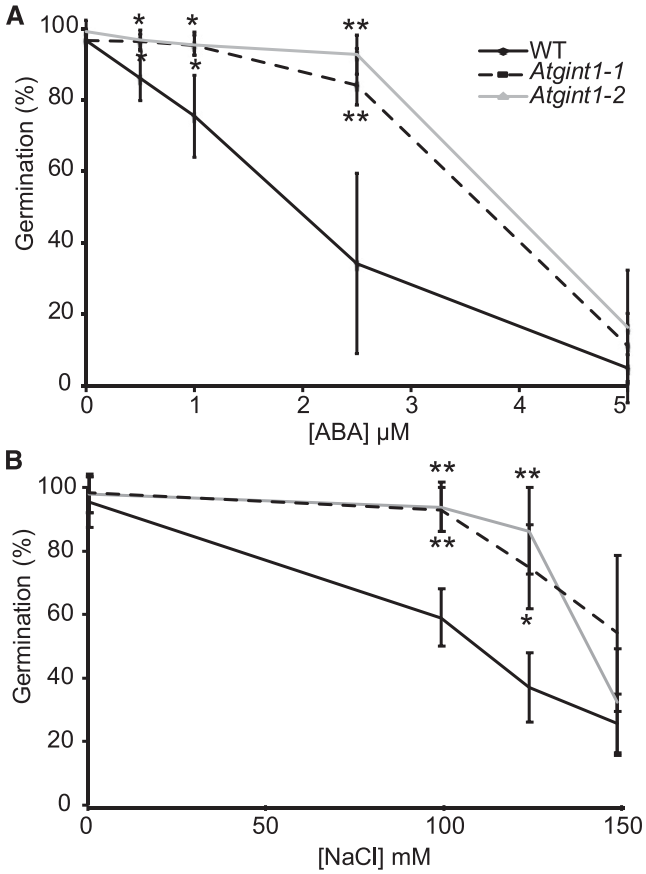

Figure 8. Effect of ABA and NaCl on wild-type and *Atgint1* seed germination. A, Seed germination rates in the presence of ABA; seeds were scored for radicle emergence after 3 d. B, Seed germination rates in the presence of NaCl, with seeds scored for radicle emergence after 2 d. Data are means of three biological replicates (>50 seeds per replicate) ± SD. An asterisk indicates statistically significant difference from the wild type (Student's *t* test, $*P < 0.05$, $**P < 0.01$).

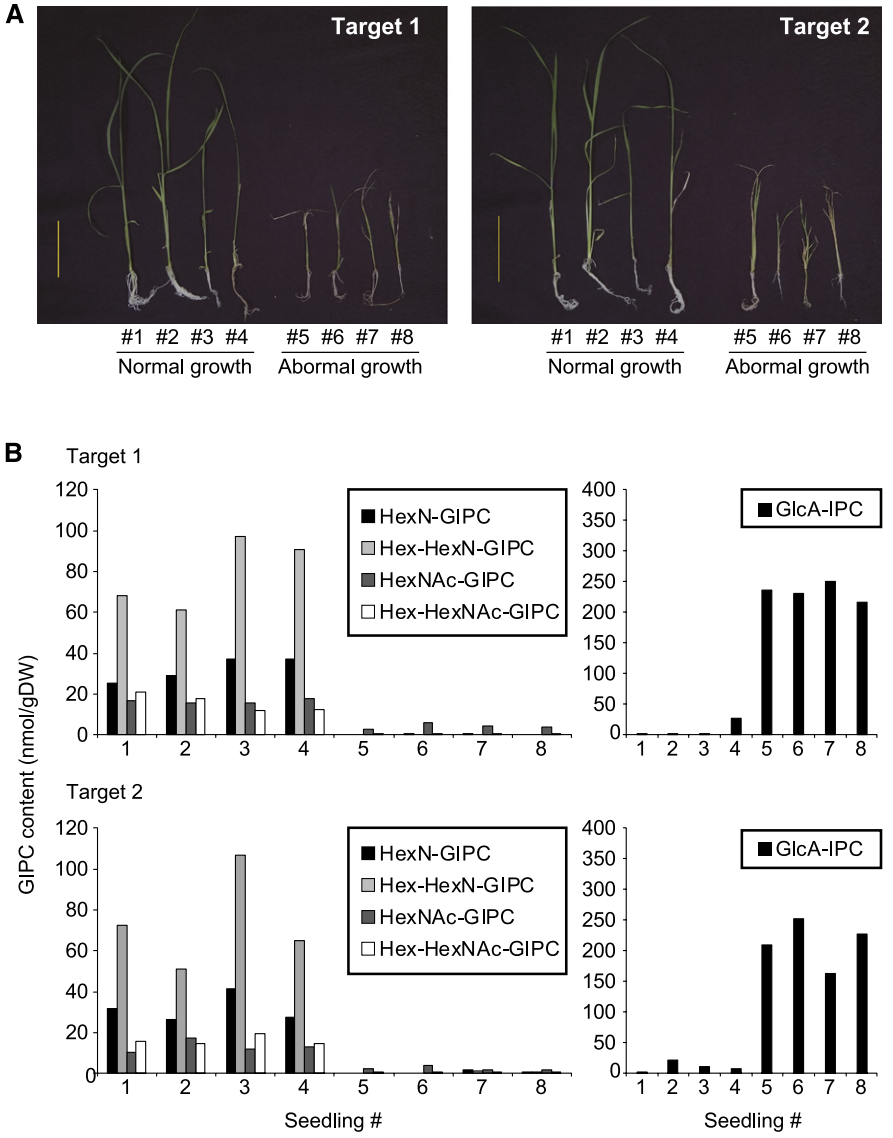

Figure 9. Seedling phenotype and GIPC content of *OsGINT1*-targeted CRISPR/Cas9 rice. A, Regenerated T0 shoots harboring T-DNA with two independent CRISPR/Cas9 *OsGINT1* target sequences were further cultured on 0.5× Murashige and Skoog media for 2–3 weeks. Some of the regenerated lines showed severely retarded growth (#5–8), which later proved to be seedling lethal. B, The GIPC content for each shoot shown in A as determined by LC-MS/MS. Hex-containing GIPCs were not detected.

Complementation of *Atgmt1* by *GINT1* Expression

Our observations demonstrate that both Hex- and HexN(Ac)-GIPCs are crucial for plant development in a plant species- and tissue-specific manner. This raises the question as to whether the two headgroup sugars have common or distinct functions. To evaluate this, the *Atgmt1* mutant was complemented by expression of either *AtGMT1*, *AtGINT1*, or *OsGINT1* driven by $35S_{pro}$. Since homozygous *Atgmt1* plants have severely compromised growth and fertility, heterozygous plants were transformed with the constructs, and lines homozygous for the loss of a functional copy of *AtGMT1* were selected in the T1 and T2 generation (Fig. 10). As expected, both the growth (Fig. 10A) and the GIPC profile (Fig. 10C) of *Atgmt1* were fully rescued by expression of $35S_{pro}$*:AtGMT1*. This contrasted with the $35S_{pro}$*:AtGINT1* and $35S_{pro}$*:OsGINT1* lines, which only partially restored the *Atgmt1* growth phenotype (Fig. 10A). The $35S_{pro}$*OsGINT1* lines exhibited slightly increased growth compared to the $35S_{pro}$*:AtGINT1* lines, which seems parallel to the metabolic complementation rate of HexN(Ac)-GIPC (Fig. 10C). It should also be noted though that the ratio of HexN-GIPC and HexN(Ac)-GIPC was different between the *AtGINT1* and *OsGINT1* overexpression lines. Taken together, these data indicate that the two different monosaccharides can only partially substitute for each other's function.

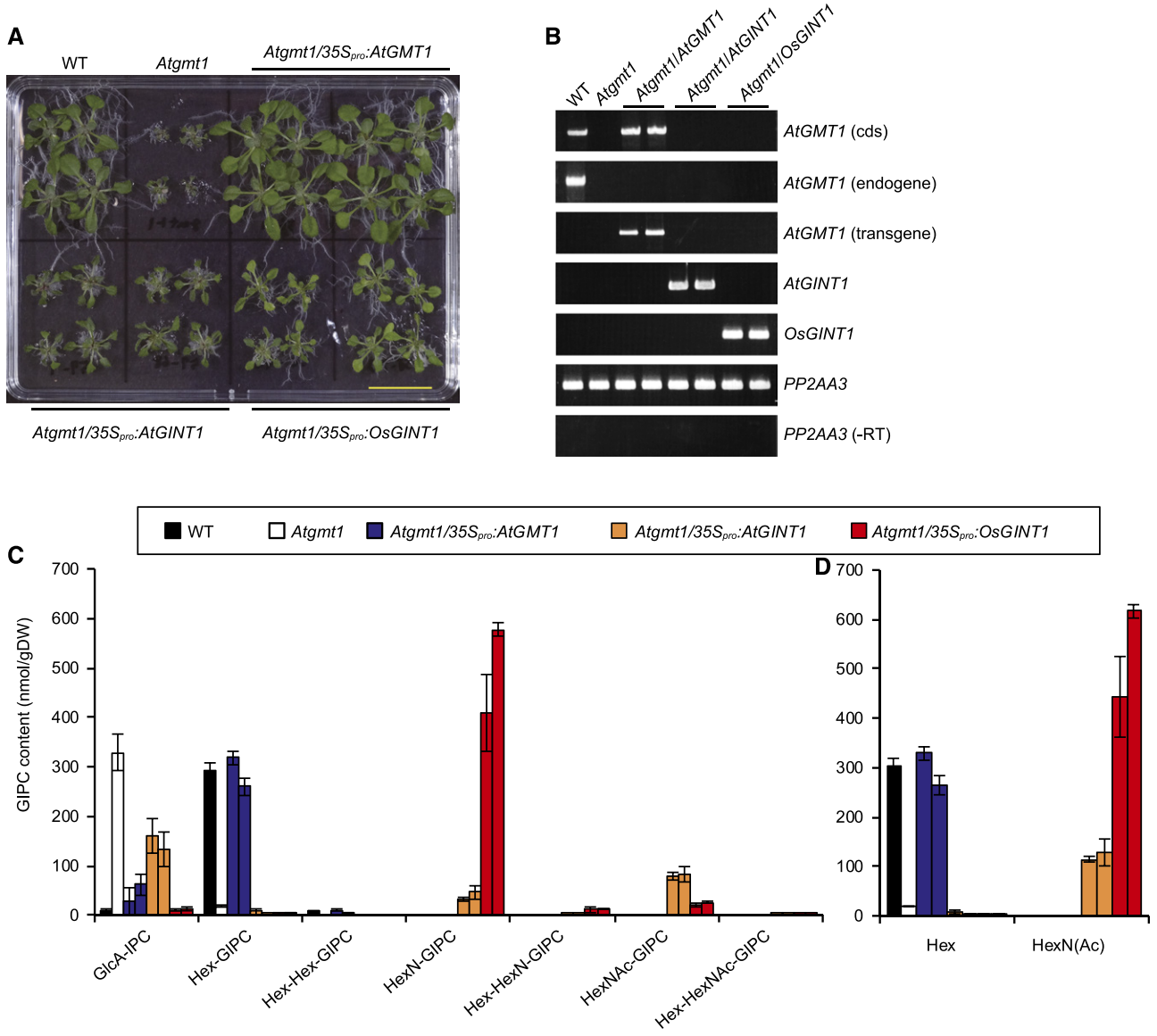

Figure 10. Heterologous complementation of *Atgmt1* with *GINT1*. A, Heterozygous *Atgmt1* plants were transformed with CaMV *35S$_{pro}$:AtGMT1*, *35S$_{pro}$:AtGINT1*, or *35S$_{pro}$:OsGINT1*. Bar = 2 cm. T2 seedlings (two independently transformed lines per construct) were analyzed by RT-PCR (B). Sphingolipidomic analyses using LC-MS/MS (C and D). C, Profiles of all the major classes of GIPCs detected in the tissues tested, and D, amounts of either Hex$_n$-only GIPCs (Hex) or HexN(Ac)-containing GIPCs [HexN(Ac)]. *PP2AA3*, *PROTEIN PHOSPHATASE 2A SUBUNIT A3*; –RT, reaction lacking reverse transcriptase enzyme. Data are means of three biological replicates (>50 seeds per replicate) ± SD.

DISCUSSION

GIPCs are critical for plant growth and development (Wang et al., 2008; Mortimer et al., 2013; Rennie et al., 2014; Fang et al., 2016; Tartaglio et al., 2017). However, their synthesis and function are poorly understood, particularly of the glycan headgroup. Identification of the enzymes responsible for glycosylation of these lipids will provide some of the tools necessary to investigate GIPC function.

Here, we have identified and characterized a GT, GINT1, which we propose is responsible for the addition of GlcNAc to the glycan headgroup of GIPCs in Arabidopsis and rice. GINT1 is a member of CAZy family GT64, and a homolog of GMT1, which we previously identified as the GIPC mannosyl transferase. Production of HexN(Ac)-GIPCs in imbibing Arabidopsis seeds follows the expression of *AtGINT1*, and Arabidopsis plants lacking a functional copy of *GINT1* do not produce detectable HexN(Ac)-GIPCs. The dominant GIPCs in Arabidopsis (Hex-GIPCs) were unaffected. Both *AtGINT1* and *OsGINT1* restored the loss of HexN(Ac)-GIPCs in *Atgint1* when expressed under the *AtGINT1* promoter, unlike *AtGMT1*. Whereas

in this report we did not show the in vitro activity for AtGINT1 or OsGINT1, constitutive expression of *GINT1* in Arabidopsis results in the de novo production of HexN(Ac)-GIPCs in leaves. Tobacco, like rice, lacks Hex-GIPCs (Carter et al., 1958; Kaul and Lester, 1975; Hsieh et al., 1981; Buré et al., 2011). Previously, we have also overexpressed *AtGINT1* in tobacco BY2 cells, and again, we did not see the production of Hex-GIPCs, whereas overexpression of AtGMT1 produced significant quantities (Fang et al., 2016). Together, these data show that, in planta, GINT1 and AtGMT1 have different substrate specificities but can use the same acceptors (GlcA-IPCs).

Considering the tissue-specific distribution of the HexN(Ac)-GIPCs in Arabidopsis, we explored whether the loss of this entire class of GIPCs in *Atgint1* affected seed development and germination. Unexpectedly, *Atgint1* seeds developed and germinated normally, although they were slightly, but significantly, larger than those of the wild type. However, the germination rate of *Atgint1* seeds was significantly less sensitive to the presence of exogenous ABA or salt. Previously, it has been reported that plants with disrupted sphingolipid biosynthesis have altered responses to ABA, including reduced sensitivity to ABA-dependent stomatal closure and suppression of germination (Ng et al., 2001; Coursol et al., 2003; Worrall et al., 2008; Wu et al., 2015). Therefore, analogous to their role in mammalian systems, sphingolipid molecules such as sphingosine-1-phosphate and ceramide may act as signaling molecules. Our data suggest that the structure of the glycan headgroup of GIPCs is also involved in ABA responses, at least in the seed. How this could be mediated is unclear, but detergent-resistant membrane fractions are highly enriched in GIPCs (Borner et al., 2005; Cacas et al., 2016). It has been proposed that the extended length of the acyl chain in GIPCs is critical both for plasma membrane microdomain stability and for defining a specific endomembrane trafficking pathway (Markham et al., 2011; Cacas et al., 2016). Altered GIPC headgroup glycosylation results in a constitutive defense response mediated by increased salicylic acid biosynthesis (Mortimer et al., 2013; Fang et al., 2016; Tartaglio et al., 2017), as well as a decrease in cellulose content (cellulose biosynthesis also occurs at the plasma membrane). Therefore, we conclude that there is evidence that the mis-glycosylation of GIPCs impacts plasma-membrane-regulated physiological processes, particularly those, such as signaling, which are often associated with lipid microdomains.

Rice vegetative tissue does not contain detectable Hex-GIPCs (Ishikawa et al., 2016) despite the presence of a *GMT1* ortholog; therefore, we hypothesized that HexN(Ac)-GIPCs may have a critical role in all tissues, in much the same way as Hex-GIPCs have in Arabidopsis. Inactivation of the rice *AtGINT1* ortholog, *OsGINT1*, resulted in abnormal growth phenotypes in seedlings regenerated from calli, which were eventually seedling lethal. These seedlings almost completely lacked HexN(Ac)-GIPCs and accumulated the substrate of OsGINT1, GlcA-IPC, to very high levels. This reinforces the data showing that *OsGINT1* can complement *Atgint1*, and strongly supports our conclusion that these enzymes have the same biochemical function in planta.

Since the distribution of HexN(Ac)-containing GIPCs is very different in rice and Arabidopsis, the characterization of GINT1 provided an opportunity to test the effects of de novo synthesis of atypical GIPC glycans on plant growth and development. Our data show that replacing a Man with a glucosamine can only partially rescue the *Atgmt1* phenotype. This implies that the identity of the sugar, as well as the sugar chain length, is important for GIPC function, depending on the tissue and species context. Alternatively, the Man-GlcA-IPC may be an important substrate for some further glycosylation steps, and these unusual longer headgroups could have specialized functions.

In line with previous studies on Arabidopsis (Mortimer et al., 2013; Fang et al., 2016), rice cells with altered GIPC headgroup structures grew normally as calli on callus-induction medium (solid and liquid), but when seedlings were regenerated or grown from seed, a severe or lethal phenotype was observed. This suggests a possible role in cell adhesion or differentiation for the GIPC headgroup, perhaps via interaction with cell wall polysaccharides, as has been proposed previously (Voxeur and Fry, 2014). Indeed, the *Atgmt1* mutant was initially identified as a cell adhesion mutant (Singh et al., 2005), and a *Volvox carteri* mutant lacking a GONST1 homolog is unable to undergo inversion at the end of embryogenesis (Ueki and Nishii, 2009). In mammalian systems, carbohydrate-carbohydrate interactions, such as Lewis^x-Lewis^x (where Lewis^x is the terminal Gal-Fuc-GlcNAc trisaccharide decorating many surface glycoproteins and glycolipids) have been shown to play a role in cell adhesion (Zhang et al., 2016). The plants developed in this publication will be used to further explore this hypothesis.

Studies using tobacco and bean have reported that the HexN(Ac) is GlcN(Ac) and that the hexose is Gal and/or Man (Carter et al., 1958; Carter and Koob, 1969). We have previously reported that the first hexose on Arabidopsis Hex-GIPCs is Man (Mortimer et al., 2013; Fang et al., 2016). However, in this study, due to the use of MS, we have referred to the GIPCs as HexN(Ac)-GIPCs and Hex-HexN-GIPCs, as we have not identified the sugars beyond their masses. Nevertheless, GlcN(Ac) is the only amino sugar known to be present in plants, and previous reports have identified GlcNAc in GIPCs from rice vegetative tissue (Kojima et al., 1991) and Arabidopsis seeds (Luttgeharm et al., 2015) is GlcN(Ac). The identity of the Hex is unknown. We predict that GINT1 transfers GlcNAc rather than GlcN, since the donor UDP-GlcNAc is abundant in plants but UDP-GlcN has not yet been detected (Ito et al., 2014). Thus, the different ratio of HexN- and HexNAc-GIPC between AtGINT1- and OsGINT1-expressing *gmt1* leaves (Fig. 10) was possibly due to a deacetylation reaction, for which the responsible enzyme remains unidentified.

To conclude, we propose that GINT1 is a GIPC α-GlcNAc transferase that likely uses UDP-GlcNAc as substrate. GlcN(Ac)-containing GIPCs are essential for rice but have a minor role in seed development and germination in Arabidopsis. We also showed that the identity of the monosaccharides on the GIPC headgroup and not just the presence of a certain number of sugar units, are important for function. This implies that there is some recognition of these structures by the plant and a potential signaling role for glycosylated GIPCs.

MATERIALS AND METHODS

Bioinformatics

Plant GT64 family genes were searched by BLAST in the Phytozome database (https://phytozome.jgi.doe.gov) for Arabidopsis (*Arabidopsis thaliana*), rice (*Oryza sativa*), moss (*Physcomitrella patens*), liverwort (*Marchantia polymorpha*), and green alga (*Chlamydomonas reinhardtii*), and the NCBI database (http://www.ncbi.nlm.nih.gov/BLAST/) for charophyte (*Klebsormidium flaccidum*). The amino acid sequences were aligned by ClustalW (http://www.genome.jp/tools-bin/clustalw), and the phylogenetic tree was constructed using NJPLOT software (Perrière and Gouy, 1996).

Sample Collection

For all experiments, unless explicitly stated, one biological replicate represents a pool of plants grown at the same time, alongside their respective control.

Plant Growth Conditions

Arabidopsis seeds were surface sterilized and sown on solid medium containing 0.5× Murashige and Skoog salts including vitamins and 1% (w/v) Suc. Following stratification (48 h, 4°C, in the dark), plates were transferred to a growth room (22°C, 100–200 µmol m^{-2} s^{-1}, 14 h light/10 h dark, 60% humidity). After 2 to 3 weeks, plants were transferred to soil.

For analyses of gene expression and GIPC profiles during seed germination, dry seeds (day 0) were imbibed for 2 d in the dark at 4°C (day 2) and incubated on Murashige and Skoog medium for 3 and 7 d (days 5 and 9) under continuous light at 22°C. Whole-plant tissues including seed coats and germinating seedlings were collected at each time point and used for RT-qPCR and GIPC analyses as follows.

GUS Staining

The 5′ flanking region with a part of N-terminal coding sequence (10 amino acids) of *AtGINT1* (−2,016 to +30) and *AtGMT1* (−1,052 to +30) was amplified by genomic PCR and cloned into pDONR207 by BP reaction (Thermo Fisher Scientific). The fragments were transferred to pMDC164 (Curtis and Grossniklaus, 2003) and used for *Agrobacterium tumefaciens*-mediated transformation of Arabidopsis. GUS staining was performed using tissues of homozygous T3 plants from at least five independent lines as described by Kawai-Yamada et al. (2009).

RT-qPCR

Total RNA was extracted from dry seeds and germinating seedlings as described by (Meng and Feldman, 2010). In brief, plant materials were ground in liquid nitrogen with a mortar and pestle and homogenized in extraction buffer (100 mM Tris-HCl, pH 9.5, 150 mM NaCl, 1% [w/v] sarkosyl, 1% [v/v] 2-mercaptoethanol). Insoluble materials were removed by centrifugation (15,000*g*, 5 min), and the supernatant was washed with 0.5 volumes each of chloroform and phenol. After centrifugation, the upper layer was collected and mixed with 0.1 volumes of 3 M sodium acetate (pH 5.2) and 0.75 volumes of 2-propanol. After incubation (10 min) and centrifugation, the supernatant was removed, and the pellet was washed with 70% (v/v) ethanol and briefly air dried. The pellet was resuspended in TRIzol reagent (Life Technologies), and total RNA was prepared according to the manufacturer's protocol. cDNA was prepared using High Capacity cDNA reverse transcription kit (Applied Biosystems), and qPCR was conducted with Power SYBR Green PCR Master Mix and a 7300 real-time PCR system (Applied Biosystems). *PP2AA3* was used as a reference. Primer sequences are shown in Supplemental Table S2.

GIPC Analysis

Lyophilized plant tissues (5–10 mg) were homogenized in 450 µL of methanol/1-butanol (1:2, v/v). After heat-denaturation of enzymes at 80°C for 10 min, 300 µL of 1 N KOH was added. The mixture was further incubated at 60°C for 30 min to eliminate glycerolipids. The extract was then acidified with 1.5 mL of 0.4 N HCl and extracted with additional 1 mL 1-butanol. After vigorous shaking and centrifugation, the upper 1-butanol layer was collected and evaporated. The residue was dissolved in 150 µL of THF/methanol/water (2:1:2, v/v/v) containing 0.1% formic acid and GIPC composition was analyzed by LC-MS/MS according to previous reports (Fang et al., 2016; Ishikawa et al., 2016).

Mutant Identification

Seeds of AT5g04500 T-DNA mutants were obtained from the Arabidopsis Biological Resource Center (*gint1-1*, SALK_002825C and *gint1-2*, GK_834G06), which are both ecotype Col-0. Plants homozygous for the T-DNA insertion were identified by PCR (Phire Plant Direct PCR kit; Finnzymes), and the site of insertion was confirmed by sequencing. RT-PCR was used to test whether the alleles were transcriptionally null as follows: Total RNA was extracted from green siliques using the RNeasy Plant Mini Kit (Qiagen). RNA was first treated with DNase I (Qiagen) and first-strand cDNA synthesis was performed using the SuperScript II RT (Life Technologies). *ACTIN7* was used as an internal control. All primers used in this study are listed in Supplemental Table S2.

Promoter Swap and Complementation of *gint1*

Genomic fragment of *AtGINT1* including 5′ upstream (2,016 bp) and 3′ downstream (710 bp) of the coding sequence was amplified by PCR. For the promoter exchange, the 5′ and 3′ sequences of *AtGINT1* were separately amplified and joined to the coding sequence of *AtGMT1* or *OsGINT1* by overlap extension PCR to prepare the chimeric complementation construct. These fragments were cloned into pDONR207 and transferred into pMDC99 (Curtis and Grossniklaus, 2003) by the Gateway system and used for transformation of *gint1*. Seeds obtained from homozygous T2 plants were used for GIPC analysis.

Seed Weight, Storage Lipid, and Protein Content

Seed weight was measured using around 200 seeds. Storage lipids were extracted by the Bligh-Dyer method (Bligh and Dyer, 1959) and subjected to methanolysis using 5% (w/v) HCl in methanol (100°C, 2 h). Margaric acid (17:0) was added as an internal standard prior to methanolysis. Fatty acid methyl esters were quantified by gas chromatography-mass spectrometry (GCMS2010; Shimadzu) using a TC-70 column (30 m × 0.25 µm × 0.25 µm; GL Science) held at 120°C for 3 min, increased to 240°C by 6°C/min and held for 5 min. Temperature of injector, interface, and ion source were kept at 250°C. Carrier gas was He at 30 cm/s. MS scan range was m/z 50 to 400 monitored between 7 and 25 min. Seed storage proteins were extracted by homogenizing seeds in Tris-buffered saline (50 mM Tris-HCl, pH 7.4, and 150 mM NaCl) and quantified with Bio-Rad protein assay kit using bovine serum albumin as a standard. Seed grain numbers used for lipid and protein analyses were counted and the contents were expressed as amount of lipids or proteins per seed grain.

Ruthenium Red Staining

Seed coat mucilage was visualized by ruthenium red staining as described by Western (2011). Dry seeds were hydrated in 50 mM EDTA for 2 h with vigorous shaking and stained with 0.01% (w/v) ruthenium red for 1 h. Seeds were washed with water and observed under a microscope.

Scanning Electron Microscopy

Scanning electron microscopy of seed surface of *gint1* mutants was performed with a TM-1000 Miniscope (Hitachi).

TEM

Arabidopsis seeds were sterilized with 10% (v/v) household bleach and imbibed overnight in distilled water at 4°C. The following day, a slit was carefully cut in the seed coat to help aid infiltration, followed by fixation in 0.1 M cacodylate buffer (pH 7.2) containing 2% (v/v) EM-grade glutaraldehyde, with gentle pulling under vacuum for 30 s. Seeds remained in fixation buffer overnight at 4°C. Seeds were rinsed three times with 0.1 M cacodylate buffer (pH 7.2), stained for 1 h with 1% (w/v) osmium tetraoxide, rinsed three times with buffer, followed by an additional three rinses with distilled water. Seeds were then dehydrated in an acetone gradient (35/50/70/80/95/100/100% v/v) and infiltrated in acetone:epon resin at 2:1, 1:1, and 1:2 dilution ratios for 1 h each, followed by pure epon resin that was freshly changed after 1 h and allowed to infiltrate overnight. The following day, seeds were infiltrated with pure resin + accelerator for 2 h and embedded in Pelco molds containing fresh resin + accelerator, which were left in a 65°C oven to polymerize for 2 d. Ultra-thin 70-nm-thick sections were collected on to grids using a diamond knife and Reichert microtome. Grids were stained with 2% (v/v) aqueous uranyl acetate for 5 min, rinsed with distilled water five times, stained with lead citrate for 5 min, and rinsed another five times with distilled water using a Pelco Grid Staining System. Grids were imaged using a Technai 1200 electron microscope. For consistency, we analyzed two grids per seed, using a total of three seeds per genotype.

AIR Cell Wall Preparation

Plant tissues (lower half of the inflorescence stems [8-week-old plants], young leaves [15-d-old plants], and dry seeds) were harvested and incubated in 96% (v/v) ethanol for 30 min at 70°C to inactivate cell wall degrading enzymes. The tissue was homogenized using a Retsch mixer mill and centrifuged at 4,000*g* for 15 min. The pellet was washed with 100% ethanol and twice with chloroform:methanol (2:1), followed by three successive washes with 65% (v/v), 80% (v/v), and 100% ethanol. The pellet was air-dried overnight. The starch in the samples was degraded with α-amylase, amyloglucosidase, and pullulanase (Megazyme) as described previously (Harholt et al., 2006). The destarched residue is referred to as AIR.

Cell Wall Monosaccharide Composition

AIR (5 mg) was hydrolyzed with fresh 2 M TFA at 121°C for 1 h. The supernatant was retained, dried under vacuum, and resuspended in 1 mL water. To release the Glc from the crystalline cellulose fraction, the TFA-insoluble material was washed with water and further hydrolyzed with 72% (v/v) sulfuric acid containing 10 µg *myo*-inositol for 1 h at room temperature. The sulfuric acid was then diluted to 1 M with water, and following incubation at 100°C for 3 h, neutralized with $BaCO_3$. All samples were filtered through a 96-well 0.45 µm filter plate (Millipore) and analyzed by high-performance anion-exchange chromatography on an ICS-5000 instrument (Thermo Fisher Scientific) equipped with a CarboPac PA20 (3 mm × 150 mm; Thermo Fisher Scientific) analytical anion-exchange column, PA20 guard column (3 mm × 30 mm), borate trap, and a pulsed amperometric detector using the elution profile described (Fang et al., 2016).

Germination Rate

Surface sterilized seeds were sowed on solid 0.5× Murashige and Skoog salt media containing either ABA (mixed isomers; Sigma-Aldrich A1049) or NaCl. Following stratification for 48 h (dark, 4°C), plates were moved to the light, and seeds were scored for radicle emergence daily. Each genotype was sown in triplicate (80–100 seeds from an individual plant per petri dish).

Embryo Characterization

For phenotypic analysis of *Atgint1* embryos, mature green siliques were dissected onto a slide and examined using a light microscope. The ratio of green (healthy) to white (arrested development) embryos was tallied.

Seed Aging

An accelerated seed aging test was performed as described by Sattler et al. (2004). Dry seeds were treated with 100% relative humidity in a tight-closed container at 40°C for 3 d and germinated on Murashige and Skoog media under continuous light at 22°C. Nontreated dry seeds were used as control. Germination rate was counted daily for 7 d.

CRISPR/Cas9-Mediated Mutagenesis of *OsGINT1*

Two target sequences for CRISPR/Cas9-mediated mutagenesis of *OsGINT1* were designed using the CRISPR-P tool (Lei et al., 2014; Supplemental Fig. S9). Each fragment was ligated to the *Bbs*I site of the pU6gRNA plasmid. The $OsU6_{pro}$*::gRNA::polyT* cassette was digested by *Asc*I and *Pac*I and introduced into pZH_gYSA_MMCas9 (Mikami et al., 2015). The binary plasmid was used for *A. tumefaciens*-mediated transformation of rice calli (Toki et al., 2006). Hygromycin-resistant calli were subcultured three to four times and transferred to regeneration medium (Murashige and Skoog salts containing vitamins, 3% [w/v] Suc, 3% [w/v] sorbitol, 0.4% [w/v] casamino acid, 2 µg/L 1-naphthaleneacetic acid, 2 mg/L kinetin, 30 mg/L hygromycin). After 2 to 3 weeks on regeneration media, emerging shoots (1–3 cm) were transferred to hormone-free rooting medium (0.5× Murashige and Skoog salts containing vitamins, 1% [w/v] Suc, 30 mg/L hygromycin) and further cultured for 2 to 3 weeks (28°C, 300 µmol m^{-2} s^{-1}, 12 h light/12 h dark). Some of the regenerated shoots showed retarded growth and finally died, although the most were grown well without dead tissues. Four independent shoots showing the typical growth phenotype were used for GIPC analysis.

Heterologous Complementation of *Atgmt1*

Full coding sequences of *AtGMT1*, *AtGINT1*, and *OsGINT1* were introduced into pH2GW7 (Karimi et al., 2002) for $CaMV35S_{pro}$-driven constitutive expression (Supplemental Fig. S3). *AtGMT1/Atgmt1* heterozygotes were transformed with the constructs and hygromycin-resistant T1 plants were selected. Homozygous *Atgmt1* mutants complemented with the transgene were screened in the T1 and T2 generations by genomic PCR and used for RT-PCR and GIPC analyses.

Accession Numbers

Sequence data from this article can be found in the GenBank/EMBL data libraries under accession numbers NM_120532.3 and AP014961.1.

Supplemental Data

The following supplemental materials are available.

Supplemental Figure S1. Phylogenetic tree of the plant GT64 family.

Supplemental Figure S2. Expression profile of *AtGINT1*.

Supplemental Figure S3. Summary of *Atgint1* alleles and constructs used in this study.

Supplemental Figure S4. GlcCer and Cer content in *Atgint1* tissues.

Supplemental Figure S5. *AtGMT1* expression in the dry seeds of *Atgint1* mutants.

Supplemental Figure S6. Noncellulosic monosaccharide composition of *Atgint1* stem and young leaf AIR.

Supplemental Figure S7. Seed longevity assay.

Supplemental Figure S8. Expression profile of *OsGINT1*, *OsGINT2*, and *OsGMT1* across development.

Supplemental Figure S9. Target sequences of CRISPR/Cas9-mediated mutagenesis of *OsGINT1*.

Supplemental Figure S10. Shoot regeneration phenotype of *Atgmt1* mutant.

Supplemental Table S1. Embryo lethality rate in *Atgint1* green siliques.

Supplemental Table S2. Primers used in this study.

Supplemental Data Set 1. Sphingolipidomic data underlying Figures 2, 3, 9, and 10.

Supplemental Data Set 2. Monosaccharide composition data underlying Figure 7 and Supplemental Figure S6.

ACKNOWLEDGMENTS

We thank Dr. Masaki Endo, Dr. Seiichi Toki (National Food Research Institute, NARO), and Mr. Masafumi Mikami (Yokohama City University) for providing CRISPR/Cas9 vectors. We thank Dr. Mi-Yeon Lee for assistance with maintaining the plant growth facilities and Dr. Jonathan Markham for advice on Arabidopsis seed GIPC analysis.

Received April 2, 2018; accepted May 1, 2018; published May 14, 2018.

LITERATURE CITED

Bligh EG, Dyer WJ (1959) A rapid method of total lipid extraction and purification. Can J Biochem Physiol **37**: 911–917

Borner GH, Sherrier DJ, Weimar T, Michaelson LV, Hawkins ND, Macaskill A, Napier JA, Beale MH, Lilley KS, Dupree P (2005) Analysis of detergent-resistant membranes in Arabidopsis. Evidence for plasma membrane lipid rafts. Plant Physiol **137**: 104–116

Buré C, Cacas JL, Wang F, Gaudin K, Domergue F, Mongrand S, Schmitter JM (2011) Fast screening of highly glycosylated plant sphingolipids by tandem mass spectrometry. Rapid Commun Mass Spectrom **25**: 3131–3145

Busse-Wicher M, Wicher KB, Kusche-Gullberg M (2014) The exostosin family: proteins with many functions. Matrix Biol **35**: 25–33

Cacas J-L, Buré C, Grosjean K, Gerbeau-Pissot P, Lherminier J, Rombouts Y, Maes E, Bossard C, Gronnier J, Furt F, (2016) Revisiting plant plasma membrane lipids in tobacco: A focus on sphingolipids. Plant Physiol **170**: 367–384

Carter HE, Koob JL (1969) Sphingolipids in bean leaves (*Phaseolus vulgaris*). J Lipid Res **10**: 363–369

Carter HE, Gigg RH, Law JH, Nakayama T, Weber E (1958) Biochemistry of the sphingolipides. XI. Structure of phytoglycolipide. J Biol Chem **233**: 1309–1314

Coursol S, Fan LM, Le Stunff H, Spiegel S, Gilroy S, Assmann SM (2003) Sphingolipid signalling in Arabidopsis guard cells involves heterotrimeric G proteins. Nature **423**: 651–654

Curtis MD, Grossniklaus U (2003) A gateway cloning vector set for high-throughput functional analysis of genes in planta. Plant Physiol **133**: 462–469

Dunn TM, Lynch DV, Michaelson LV, Napier JA (2004) A post-genomic approach to understanding sphingolipid metabolism in *Arabidopsis thaliana*. Ann Bot **93**: 483–497

Fang L, Ishikawa T, Rennie EA, Murawska GM, Lao J, Yan J, Tsai AY, Baidoo EE, Xu J, Keasling JD, (2016) Loss of inositol phosphorylceramide sphingolipid mannosylation induces plant immune responses and reduces cellulose content in Arabidopsis. Plant Cell **28**: 2991–3004

Finn RD, Attwood TK, Babbitt PC, Bateman A, Bork P, Bridge AJ, Chang HY, Dosztányi Z, El-Gebali S, Fraser M, (2017) InterPro in 2017-beyond protein family and domain annotations. Nucleic Acids Res **45**: D190–D199

Harholt J, Jensen JK, Sørensen SO, Orfila C, Pauly M, Scheller HV (2006) ARABINAN DEFICIENT 1 is a putative arabinosyltransferase involved in biosynthesis of pectic arabinan in Arabidopsis. Plant Physiol **140**: 49–58

Hsieh TC, Lester RL, Laine RA (1981) Glycophosphoceramides from plants. Purification and characterization of a novel tetrasaccharide derived from tobacco leaf glycolipids. J Biol Chem **256**: 7747–7755

Ishikawa T, Ito Y, Kawai-Yamada M (2016) Molecular characterization and targeted quantitative profiling of the sphingolipidome in rice. Plant J**88**: 681–693

Ito J, Herter T, Baidoo EE, Lao J, Vega-Sánchez ME, Michelle Smith-Moritz A, Adams PD, Keasling JD, Usadel B, Petzold CJ, (2014) Analysis of plant nucleotide sugars by hydrophilic interaction liquid chromatography and tandem mass spectrometry. Anal Biochem **448**: 14–22

Karimi M, Inzé D, Depicker A (2002) GATEWAY vectors for Agrobacterium-mediated plant transformation. Trends Plant Sci **7**: 193–195

Kaul K, Lester RL (1975) Characterization of inositol-containing phosphosphingolipids from tobacco leaves: Isolation and identification of two novel, major lipids: N-acetylglucosamidoglucuronidoinositol phosphorylceramide and glucosamidoglucuronidoinositol phosphorylceramide. Plant Physiol **55**: 120–129

Kawai-Yamada M, Hori Z, Ogawa T, Ihara-Ohori Y, Tamura K, Nagano M, Ishikawa T, Uchimiya H (2009) Loss of calmodulin binding to Bax inhibitor-1 affects Pseudomonas-mediated hypersensitive response-associated cell death in *Arabidopsis thaliana*. J Biol Chem **284**: 27998–28003

Kojima M, Ohta K, Ohnishi M, Ito S (1991) Chemical characterization of sphingophosphoglycolipids in rice leafy stems. Res. Bull. Obihiro. Univ. I **17**: 143–148

Lei Y, Lu L, Liu HY, Li S, Xing F, Chen LL (2014) CRISPR-P: a web tool for synthetic single-guide RNA design of CRISPR-system in plants. Mol Plant **7**: 1494–1496

Lenarčič T, Albert I, Böhm H, Hodnik V, Pirc K, Zavec AB, Podobnik M, Pahovnik D, Žagar E, Pruitt R, (2017) Eudicot plant-specific sphingolipids determine host selectivity of microbial NLP cytolysins. Science **358**: 1431–1434

Luttgeharm KD, Kimberlin AN, Cahoon RE, Cerny RL, Napier JA, Markham JE, Cahoon EB (2015) Sphingolipid metabolism is strikingly different between pollen and leaf in Arabidopsis as revealed by compositional and gene expression profiling. Phytochemistry **115**: 121–129

Markham JE, Jaworski JG (2007) Rapid measurement of sphingolipids from *Arabidopsis thaliana* by reversed-phase high-performance liquid chromatography coupled to electrospray ionization tandem mass spectrometry. Rapid Commun Mass Spectrom **21**: 1304–1314

Markham JE, Li J, Cahoon EB, Jaworski JG (2006) Separation and identification of major plant sphingolipid classes from leaves. J Biol Chem **281**: 22684–22694

Markham JE, Molino D, Gissot L, Bellec Y, Hématy K, Marion J, Belcram K, Palauqui JC, Satiat-Jeunemaître B, Faure JD (2011) Sphingolipids containing very-long-chain fatty acids define a secretory pathway for specific polar plasma membrane protein targeting in Arabidopsis. Plant Cell **23**: 2362–2378

Markham JE, Lynch DV, Napier JA, Dunn TM, Cahoon EB (2013) Plant sphingolipids: function follows form. Curr Opin Plant Biol **16**: 350–357

Meng L, Feldman L (2010) A rapid TRIzol-based two-step method for DNA-free RNA extraction from Arabidopsis siliques and dry seeds. Biotechnol J **5**: 183–186 10.1002/biot.20090021120108272

Mikami M, Toki S, Endo M (2015) Comparison of CRISPR/Cas9 expression constructs for efficient targeted mutagenesis in rice. Plant Mol Biol **88**: 561–572

Mortimer JC, Yu X, Albrecht S, Sicilia F, Huichalaf M, Ampuero D, Michaelson LV, Murphy AM, Matsunaga T, Kurz S, (2013) Abnormal glycosphingolipid mannosylation triggers salicylic acid-mediated responses in Arabidopsis. Plant Cell **25**: 1881–1894

Ng CK, Carr K, McAinsh MR, Powell B, Hetherington AM (2001) Drought-induced guard cell signal transduction involves sphingosine-1-phosphate. Nature **410**: 596–599

Perrière G, Gouy M (1996) WWW-query: an on-line retrieval system for biological sequence banks. Biochimie **78**: 364–369

Rennie EA, Ebert B, Miles GP, Cahoon RE, Christiansen KM, Stonebloom S, Khatab H, Twell D, Petzold CJ, Adams PD, (2014) Identification of a sphingolipid α-glucuronosyltransferase that is essential for pollen function in Arabidopsis. Plant Cell **26**: 3314–3325

Sattler SE, Gilliland LU, Magallanes-Lundback M, Pollard M, DellaPenna D (2004) Vitamin E is essential for seed longevity and for preventing lipid peroxidation during germination. Plant Cell **16**: 1419–1432

Singh SK, Eland C, Harholt J, Scheller HV, Marchant A (2005) Cell adhesion in *Arabidopsis thaliana* is mediated by ECTOPICALLY PARTING CELLS 1—a glycosyltransferase (GT64) related to the animal exostosins. Plant J **43**: 384–397

Tartaglio V, Rennie EA, Cahoon R, Wang G, Baidoo E, Mortimer JC, Cahoon EB, Scheller HV (2017) Glycosylation of inositol phosphorylceramide

sphingolipids is required for normal growth and reproduction in Arabidopsis. Plant J **89**: 278–290

Tellier F, Maia-Grondard A, Schmitz-Afonso I, Faure JD (2014) Comparative plant sphingolipidomic reveals specific lipids in seeds and oil. Phytochemistry **103**: 50–58

Toki S, Hara N, Ono K, Onodera H, Tagiri A, Oka S, Tanaka H (2006) Early infection of scutellum tissue with Agrobacterium allows high-speed transformation of rice. Plant J **47**: 969–976

Ueki N, Nishii I (2009) Controlled enlargement of the glycoprotein vesicle surrounding a volvox embryo requires the InvB nucleotide-sugar transporter and is required for normal morphogenesis. Plant Cell **21**: 1166–1181

Voxeur A, Fry SC (2014) Glycosylinositol phosphorylceramides from Rosa cell cultures are boron-bridged in the plasma membrane and form complexes with rhamnogalacturonan II. Plant J **79**: 139–149

Wang W, Yang X, Tangchaiburana S, Ndeh R, Markham JE, Tsegaye Y, Dunn TM, Wang GL, Bellizzi M, Parsons JF, (2008) An inositolphosphorylceramide synthase is involved in regulation of plant programmed cell death associated with defense in Arabidopsis. Plant Cell **20**: 3163–3179

Western TL (2011) The sticky tale of seed coat mucilages: production, genetics, and role in seed germination and dispersal. Seed Sci Res **22**: 1–25

Winter D, Vinegar B, Nahal H, Ammar R, Wilson GV, Provart NJ (2007) An "Electronic Fluorescent Pictograph" browser for exploring and analyzing large-scale biological data sets. PLoS One **2**: e718

Worrall D, Liang Y-K, Alvarez S, Holroyd GH, Spiegel S, Panagopulos M, Gray JE, Hetherington AM (2008) Involvement of sphingosine kinase in plant cell signalling. Plant J **56**: 64–72

Wu J-X, Li J, Liu Z, Yin J, Chang Z-Y, Rong C, Wu J-L, Bi F-C, Yao N (2015) The Arabidopsis ceramidase AtACER functions in disease resistance and salt tolerance. Plant J **81**: 767–780

Zhang Y, Lu D, Sollogoub M, Zhang Y (2016) Carbohydrate-carbohydrate interaction: from hypothesis to confirmation. *In* **AR Rauter, TK Lindhorst, Y Queneau**, eds, Carbohydrate Chemistry, Vol 41. The Royal Society of Chemistry, Cambridge, pp 238–254